

# Wireless sensor nodes featuring single or double band directive antennas for agriculture applications

## Nodos sensores inalámbricos con antenas directivas de banda simple o doble para aplicaciones en agricultura

DOI: <http://doi.org/10.17981/ingecuc.16.2.2020.07>

Scientific Research Article. Date Received: 06/10/2019. Acceptance Date: 02/04/2020.

**Martha Aurora Gonzalez Jaramillo** 

Universidad Distrital Francisco José de Caldas. Bogotá, D.C (Colombia)  
magonzalezj@correo.udistrital.edu.co

**Cesar Aníbal Echeverry Moreno** 

Universidad Distrital Francisco José de Caldas. Bogotá, D.C (Colombia)  
caecheverrym@correo.udistrital.edu.co

**Carlos Arturo Suárez Fajardo** 

Universidad Distrital Francisco José de Caldas. Bogotá, D.C (Colombia)  
csuarezf@udistrital.edu.co

**Gustavo Adolfo Puerto Leguizamón** 

Universidad Distrital Francisco José de Caldas. Bogotá, D.C (Colombia)  
gapuerto@udistrital.edu.co

Para citar este artículo:

M. Gonzalez Jaramillo, C. Echeverry Moreno, C. Suárez Fajardo & G. Puerto Leguizamón “Wireless sensor nodes featuring single or double band directive antennas for agriculture applications”, *INGE CUC*, vol. 16, no. 2, pp. 104–118, 2020. DOI: <http://doi.org/10.17981/ingecuc.16.2.2020.07>

### Resumen

**Introducción**— Este artículo presenta el diseño de dos nodos de sensores inalámbricos, con sistemas de comunicaciones que integran en un caso una antena de banda ancha para operación en las bandas de 900MHz y 2.4GHz, junto con un circuito que permite seleccionar el radio apropiado para operación en alguna de estas bandas con la misma antena y el otro hace uso de una antena de alta ganancia para operación en la banda de 2.4GHz. El diseño propuesto ofrece una solución al problema de propagación de señales de Radio Frecuencia (RF) en bosques y plantaciones para aplicaciones en agricultura inteligente que hacen uso de Redes de Sensores Inalámbricos (WSN).

**Objetivo**— Diseñar dos nodos de sensores inalámbricos, con sistemas de comunicaciones que integran antenas directivas en un caso para operación en doble banda (900MHz-2.4GHz) y en el otro con antenas de alta ganancia (2.4GHz) para aplicaciones en agricultura inteligente.

**Metodología**— El diseño de los nodos inalámbricos hace uso del PSoC (Sistema Programable en Chip) modelo CY8CKIT-059 5LP, al cual se integran sensores de temperatura, humedad, inclinación, distancia, intensidad de luz y movimiento que utilizan ZigBee como protocolo de comunicación inalámbrica. Las antenas son diseñadas con simuladores electromagnéticos apropiados y los prototipos resultantes de este proceso son caracterizados en impedancia mediante un Analizador de Redes (VNA) y en diagrama en una cámara anecoica. La operación integral de los nodos se valida en el laboratorio y en espacios abiertos.

**Resultados**— El nodo de doble banda con antena logarítmica permite transferencia de paquetes a distancias de 4.1km (915 MHz) y de 938m (2.44 GHz), junto con un circuito de conmutación que permite seleccionar una de las bandas dependiendo de las características de propagación del medio donde se instalará el nodo. Por otra parte, el nodo con antena SPA permite transferencia de paquetes hasta 2.5 Km (2.44 GHz). Los resultados de la caracterización de las antenas son: La antena logarítmica presenta una ganancia máxima de 2.74 dBi (915 MHz) y 3.06d Bi (2.44 GHz) respectivamente, con un ancho de banda de impedancia de 3.196:1, para un  $S_{11} < -10\text{dB}$ . La antena SPA resuena a una frecuencia central de 2.44 GHz con una ganancia de 7.2 dBi; un ancho de banda de impedancia del 16.8%, para un  $S_{11} < -10\text{dB}$ .

**Conclusiones**— La propuesta consigue mejorar el desempeño en redes inalámbricas de sensores por su modularidad, versatilidad y su aplicación en diferentes áreas incluida la agricultura, lo que permite obtener mejores alcances y cobertura más amplia cuando se compara con los nodos que hacen uso de antenas XBee convencionales.

**Palabras clave**— Redes inalámbricas de sensores (WSN); comunicaciones inalámbricas; propagación de RF; antenas directivas; agricultura de precisión

### Abstract

**Introduction**— This paper presents the design of two wireless sensor nodes, with communications systems that integrate in one case a broadband antenna for operation in the 900MHz and 2.4GHz bands, along with a circuit that allows to select the appropriate radio for operation in some of these bands with the same antenna and the other makes use of a high gain antenna for operation in the 2.4GHz band. The proposed design offers a solution to the problem of propagation of Radio Frequency (RF) signals in forests and plantations for applications in smart agriculture that make use of Wireless Sensor Networks (WSN).

**Objective**— Design of two wireless sensor nodes, with communications systems that integrate directive antennas in one case for dual band operation (900MHz-2.4GHz) and in the other with high gain antennas (2.4GHz) for applications in smart agriculture.

**Method**— The design of the wireless nodes makes use of the PSoC (Programmable Chip System) model CY8CKIT-059 5LP, which integrates temperature, humidity, inclination, distance, light intensity and movement sensors that use ZigBee as a wireless communication protocol. The antennas are designed with appropriate electromagnetic simulators and the resulting prototypes from this process are characterized in impedance by means of a Vector Network Analyzer (VNA) and radiation patterns in an anechoic chamber. The full operation of the nodes is validated in the laboratory and in open spaces.

**Results**— The double-band node with logarithmic antenna allows packet transfer at distances of 4.1km (915 MHz) and 938m (2.44 GHz), along with a switching circuit that allows one of the bands to be selected depending on the propagation characteristics of the medium where the node will be installed. On the other hand, the node with SPA antenna allows transfer of packets up to 2.5 km (2.44 GHz). The antenna characterization results are as follows: The logarithmic antenna has a maximum gain of 2.74 dBi (915 MHz) and 3.06 dBi (2.44 GHz) respectively, with an impedance bandwidth of 3.196:1, for an  $S_{11} < -10\text{dB}$ . The SPA antenna resonates at a center frequency of 2.44 GHz with a gain of 7.2 dBi; an impedance bandwidth of 16.8%, for an  $S_{11} < -10\text{dB}$ .

**Conclusions**— This proposal improves the performance in wireless sensor networks since the approaches allow modularity, versatility and application in different areas including agriculture, enabling longer reaches and a more extensive coverage compared to the nodes that make use of conventional XBee antennas.

**Keywords**— Wireless Sensor Network (WSN); wireless communication; RF propagation; directive antennas, precision agriculture

## I. INTRODUCTION

Wireless Sensor Networks (WSN) are systems with distributed nodes that have the capability to obtain, process, storage and exchange information through wireless links to a coordinator node. These nodes are autonomous devices that have as main components: a microcontroller, a power source, a radio-transceiver (RF) and sensors [1]. Sensor networks are used in applications such as domotic, automation, industry, agriculture, medicine, environment, traffic, among others [2].

The PSoC is a digital and analog electronic processing unit based on ARM Cortex microcontrollers family. This device has favorable features hard to find in conventional microcontrollers, such as: FPGA functionalities, block-hybrid programming and C code and low cost among others [3].

Currently, there are different sensor nodes that are differentiated by energy consumption, processing, number and type of ports, sizes and scopes [4]. The main commercial nodes are: Waspote by Libelium [5], Xbee IO Pro by Olimex [6], nodes Mica, Mica2, MicaZ, Lotus and Iris by Memsic [7], Imote by Crossbow and eZ430-RF2500 by Texas instrument [8]. These nodes have ranges of operation from 50 m to 1 km in the 2.4 GHz band with omnidirectional antennas. Most of wireless sensor nodes use monopole, dipole and chip antennas operating in a single frequency band (900 MHz or 2.4 GHz) with an omnidirectional radiation pattern and gains in the order of 0.6dBi to 2.1 dBi range [9], [10], [11].

The agriculture industry has started to use Wireless Sensor Networks (WSN) in environmental monitoring and surveillance, technifying crops and bringing them into the category of smart agriculture or precision agriculture. In agricultural plantation applications, WSN is used as a means of protection and control in real time, through which it is possible to detect diseases, as well as monitor soil temperature and humidity. In this context, wireless communications systems in WSN networks for applications in forests and plantations play a key role from coverage and link quality viewpoints, which requires solving problems such as propagation losses due to soil and the reflections caused by the treetops (canopy). In such a context, there have been identified several issues to tackle e.g. the propagation models in this type of environment [12]-[14], the efficiency of wireless technologies in various environments [15], the security in these networks [16], and radio diversity for reliable communication in WSNs [17] among others.

In addition, wireless sensor nodes based on omnidirectional antennas and amplifiers with low antenna power levels, have limitations in applications such as agriculture, due to the attenuation of signals in plantations and forests [12]-[14], limiting the effectiveness of such systems. Thus, this paper presents the design and fabrication of two wireless sensor nodes, one of them includes a logarithmic broadband antenna for operation in the 900 MHz and 2.4 GHz bands along with a circuit that allows to select the appropriate radio to operate in one of these bands and the other integrates a high gain Suspended Plate Antenna (SPA) for operation in the 2.4 GHz band which allows to configure a frequency and space diversity system for reliable communication in wireless sensor networks. Therefore, the two wireless sensor nodes for WSN applications aims at improving the communications performance while reduces the power consumption.

In this context, the corresponding RF system can be selected taking into account the environment, sensor network requirements and application. While the log periodic antenna enables long distance communication links in the 900 MHz band or shorter distances at 2.4 GHz, the proposed SPA antenna presents a higher gain than commercial antennas, therefore, both solution contribute to mitigate multipath signal loss, environmental fading and interference.

The first node consists of a power source, a set of sensors, a PSoC model CY8CKIT-059, a 2.4 GHz and a 900 MHz XBee radios, a low gain dual band log-periodic antenna and the switching system. Complete detail of a wireless sensor node design using log-periodic antenna is presented in [18]. The second node integrates a 2.4 GHz XBee module connected to the high gain SPA antenna, a PSoC model CY8CKIT-059 and a sensor kit. Both modules make use of the same power source and selection of the radiating system to use can be performed at any

time. Thus, the approach improves commercial wireless sensor nodes limitations in terms of communication link reach, processing, ease programming, configuration and interoperability with different sensors.

Additionally, in the first node, the communication system is managed through the PSoC, where two communication channels were programmed for two different XBee radios and an additional output to control a SPDT (Single Pole Double Throw) radio frequency switching system achieving a dual operation in 915 MHz or 2.4 GHz with the same antenna. The second node allows the RF communication with a single radio using a high gain SPA antenna at 2.44 GHz. Thus, it is possible to program two different devices and configure them to adapt the node depending on particular environment needs.

## II. METHODOLOGY

This section describes wireless sensor node design including the sensors, PSoC features, the SPA and log periodic antenna design and prototype components.

### A. Sensor and PSOC selection

Most of common low cost sensors used in different industries such as home automation, health, industry and agriculture were employed in the designed node and are listed in [Table 1](#) [18].

TABLE 1. SELECTED SENSORS.

Sensor Reference	Manufacturer	Variable
LM35	Texas Instrument	Temperature
HIH-4000-002	Honeywell	Relative humidity
DTH11	Mybotic	Temperature and humidity
CMPS10	Robot-electronics	Compass and tilt
GP2Y0A02YK	SHARP	Infrared distance
HC-SR04	ElecFreak	Ultrasound distance
GA1A2S100SS	SHARP	Light intensity
555 28027	Parallax	Movement

Source: Adapted from [18].

In the design of nodes for wireless sensor networks is usual to use microcontrollers as processing units due to their low power consumption, easy programming and low cost. However, these qualities can be found and improved by PSoC devices, which have features such as programming in analog and digital blocks (Flip-Flops, DACs, analog multiplex, etc.), routing capacity and internal hardware interconnections (analog routing), clock rates of up to 80MHz, all these features for approximately a \$10USD price. The PSoC model CY8CKIT-059 5LP was chosen to perform the processing of analog and digital signals conveyed over different protocols [13]. The main features of this processing unit are shown in [Table 2](#) [3].

TABLE 2. MAIN FEATURES PSoC CY8CKIT-059.

Item	Value
Core	ARM Cortex-M3 - 32 bits
Speed	Until 80 MHz, 84 MIPS
Memory	*Flash: 32 KB to 256 KB *SRAM: 8 KB to 64 KB
Peripherals	I <sup>2</sup> C, SPI, UART, LIN, CAN, FS USB 2.0, I <sup>2</sup> S
# Blocks	20 a 24 UDBs
Analog-Digital Blocks	*1 Delta-Sigma ADC (8 to 20 bits) 192 ksps @ 12 bits *Until 4 DAC (8 bits)
Electric Consumption	*Operation: 2.7 V to 5.5 V *Active: 2 mA, Suspended: 2 $\mu$ A, Hibernating: 300 nA

Source: Cypress Technologies.

Three different use modes were programmed, namely: Configuration mode, Demo mode (for testing), and Operation mode. The configuration is executed using a computer with RS232 serial data protocol or through a central node allowing remote configuration. In this context, the configuration and checking of the available sensors, the internal reference time, the individual node features such as the ID and the transmission state variables such as the battery level were transmitted using RS232 protocol.

The communication system is managed through PSoC where two communication channels were programmed for two different XBee radios and an additional output to control a SPDT radio frequency switching system achieving a dual operation in 900 MHz and 2.4 GHz frequencies with the same antenna. The user can also communicate through a single radio on the node using a high gain SPA antenna at 2.44 GHz. Thus, it is possible to program two different devices and configure them to adapt the node depending on particular environment needs.

Fig. 1 shows the flow diagram of the main logic programming on the PSoC. First, the RTC and UART were initialized, after that, the mode was selected: demo, operation or configuration. The transmission frequency was set through the configuration of the SPDT. Then, the chosen sensor is measured and finally the data is wirelessly transmitted and displayed to the user.

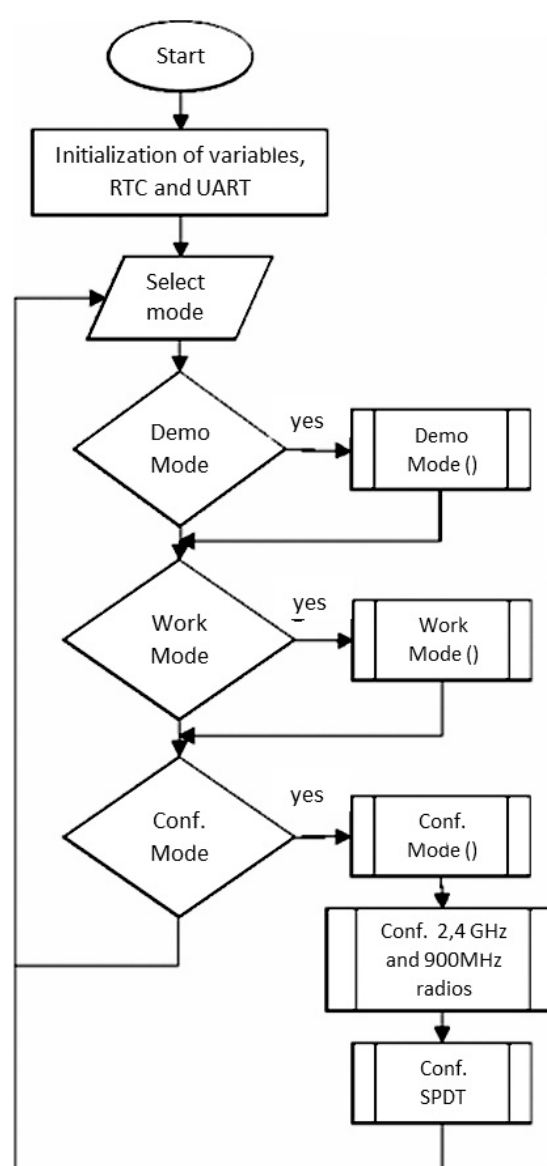


Fig. 1. Flow graph of the PSoC programming.  
Source: Authors.

### B. Antenna Design

Design equations of SPA antennas are based on a microstrip patch, for this case a square patch is designed with electrical substrate characteristics, choosing the air, its dielectric constant is  $\epsilon_r = 1$ , tangent losses  $\tan\delta = 0$  and height ( $h$ ) corresponds to the optimal suspended space according to the frequency ( $0.03\lambda - 0.12\lambda$ ) [19]. For the SPA antenna design, is necessary a ground plane, a radiant plane, an excitation and supports of low relative permittivity [20]. The equations (1)-(5) are based on [21], [22], where (1) represents patch width  $W$ , (2) defines the effective dielectric constant  $\epsilon_{r_{eff}}$ , (3) is the patch lengthening by edge effects  $\delta L$ , (4) represents the effective length  $L_{eff}$  and (5) is the length of the patch  $L$ . In these equations represents the speed of light and  $f_r$  is the central frequency.

$$W = \frac{c}{2f_r} \sqrt{\frac{2}{\epsilon_r + 1}} \quad (1)$$

$$\epsilon_{\text{reff}} = \frac{\epsilon_r + 1}{2} + \frac{\epsilon_r - 1}{2} \left[ 1 + 12 \frac{h}{W} \right]^{-\frac{1}{2}} \quad (2)$$

$$\delta L = (0.412 * h) \frac{(\epsilon_{\text{reff}} + 0.3) \left( \frac{W}{h} + 0.264 \right)}{(\epsilon_{\text{reff}} - 0.258) \left( \frac{W}{h} + 0.8 \right)} \quad (3)$$

$$L_{\text{eff}} = \frac{c}{2f_r \sqrt{\epsilon_r}} \quad (4)$$

$$L = L_{\text{eff}} - 2\delta L \quad (5)$$

Firstly, in the design process, the central frequency is established at 2.44 GHz, the reason is that XBee works in the Industrial, Scientific and Medical (ISM) spectrum band of 2.4 GHz - 2.4835 GHz. Based on the equations described above the corresponding values are calculated. Using parametric analysis on simulations, these parameters are adjusted: separation height ( $h$ ), radiant patch width ( $W$ ) and excitation point. It allows to obtain appropriate geometry for the best response in impedance coupling and gain. The final dimensions are: separation height ( $h$ ) = 10 mm, length and width of substrate ( $L$ ) = 55mm, length and width of ground plane = 70mm and excitation point is located in ( $x = 5$ ,  $y = 27.5$ ). The prototype of the SPA antenna was made in 0.5 mm copper foil, using nylon screws in order to separate the plates and a 4 mm diameter and a 1.2 mm thick copper wire as feed point was selected.

The log periodic antenna design use equations (6)-(8), these are based on [18], [23]. In this context, (6) represents the scaling factor  $\tau$ , (7) is the dipole length  $L_{\text{dip}}$  and (8) is the average impedance  $Z_a$ . In these equations,  $f$  represents frequency,  $l$  length,  $w$  width,  $s$  spacing,  $\lambda$  wavelength, and  $n$  elements number. Calculated values are:  $\tau = 0.86$  and  $n = 10$ . The dimensions of each element are:

$$l_1 = 65 \text{ mm}, w_1 = 3 \text{ mm}, s_1 = 33 \text{ mm},$$

$$l_2 = 56 \text{ mm}, w_2 = 2.5 \text{ mm}, s_2 = 28 \text{ mm},$$

$$l_3 = 48 \text{ mm}, w_3 = 2.2 \text{ mm}, s_3 = 24 \text{ mm},$$

$$l_4 = 41 \text{ mm}, w_4 = 1.9 \text{ mm}, s_4 = 21 \text{ mm},$$

$$l_5 = 35 \text{ mm}, w_5 = 1.6 \text{ mm}, s_5 = 18 \text{ mm},$$

$$l_6 = 30 \text{ mm}, w_6 = 1.4 \text{ mm}, s_6 = 15 \text{ mm},$$

$$l_7 = 26 \text{ mm}, w_7 = 1.2 \text{ mm}, s_7 = 13 \text{ mm},$$

$$l_8 = 22 \text{ mm}, w_8 = 1 \text{ mm}, s_8 = 11 \text{ mm},$$

$$l_9 = 19 \text{ mm}, w_9 = 0.9 \text{ mm}, s_9 = 10 \text{ mm},$$

$$l_{10} = 17 \text{ mm}, w_{10} = 0.8 \text{ mm}, s_{10} = 8 \text{ mm},$$

$$\tau = \frac{f_1}{f_2} = \frac{f_n}{f_{n+1}} = \frac{l_n}{l_{n+1}} = \frac{w_n}{w_{n+1}} = \frac{s_n}{s_{n+1}} \quad (6)$$

$$L_{\text{dip}} = \frac{\lambda_{\text{max}}}{2} = 2l_1 \rightarrow l_1 = \frac{\lambda_{\text{max}}}{4} \quad (7)$$

$$Z_a = 120 \left( \ln \left( \frac{l_n}{w_n} \right) - 2.25 \right) \quad (8)$$

This antenna has two symmetrical layers and reflected patches top face feed with a lag of  $180^\circ$  with respect to the underside patch. A bias was used for connection between the layers. Finally, a prototype of the antenna was made using RF30 substrate. Both antenna prototypes were characterized in impedance and pattern using a Rohde & Schwarz ZVL13 vector network analyzer and the anechoic chamber respectively.

### C. Prototype Integration

The node with the SPA antenna of square geometry has a total area of , in which its main components are included: PSoC 5LP, Xbee-Pro 802.15.4 S1, sensor terminals and 3V DC power with two AA batteries. The use of pigtailed allows connecting and stacking the antenna on the circuit. The elements were organized in a chassis: batteries in the lower side of the chassis, PCB in the middle and antenna in the upper position.

The XBee chosen was the XBee-Pro 802.15.4 S1 that operates on 2.4 GHz-2.4835 GHz bands. It has a RPSMA connector, point-to-multipoint topology, long range, low power consumption, 18dBm transmission power, 250 kbps data rate and -100dBm sensitivity. Fig. 2 shows the wireless sensor node using a SPA antenna.

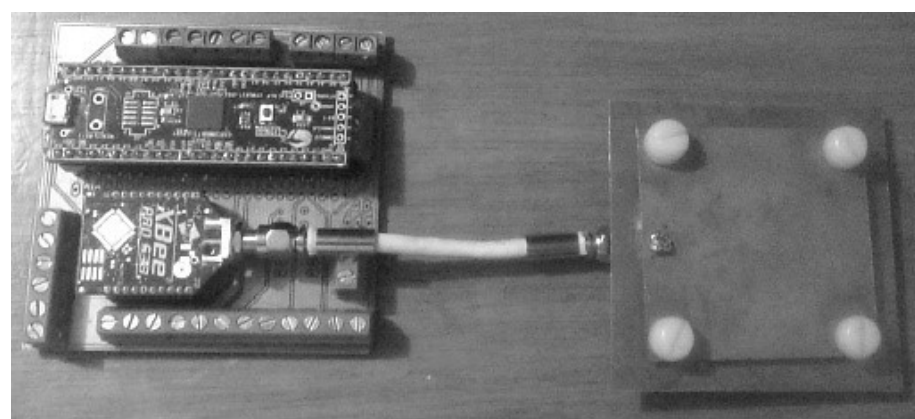


Fig. 2. Wireless sensor node with SPA antenna.  
Source: Authors.

The wireless sensor node prototype with log periodic antenna occupies a space of  $140 \times 120$  mm and has a quasi-triangle geometry, it is composed by a PSoC, an SPDT for frequency switching according to the environment and application requirements, two XBee devices: a XBee-Pro 802.15.4 S1 for 2.4 GHz band and a XBee-Pro XSC S3B for 900 MHz. The last one has 24 dBm transmission power, 20 kbps data rate and -109 dBm sensitivity. Besides, the prototype has two AA batteries and sensor terminals. Fig. 3 shows the wireless sensor node using a log periodic antenna [18].

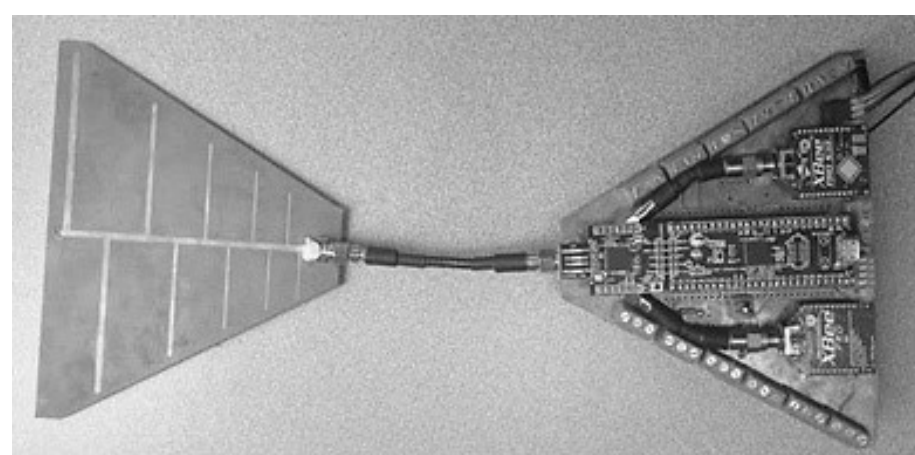


Fig. 3. Wireless sensor node with log periodic antenna.  
Source: Adapted from [18].

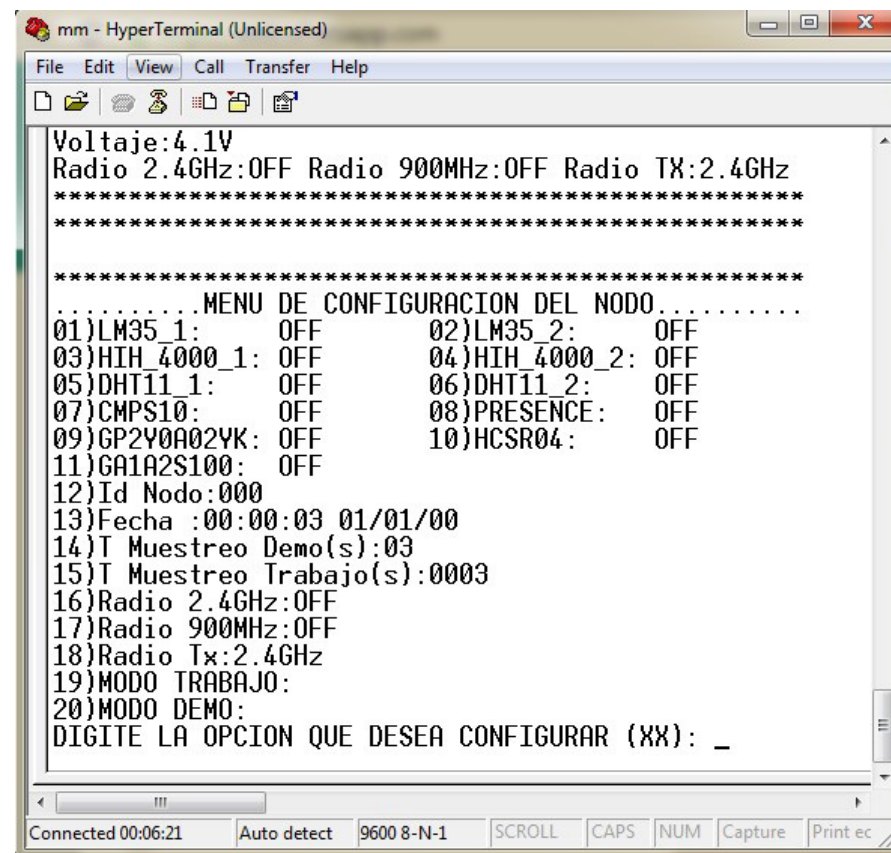
In order to determine the maximum communication distance between the proposed nodes that make use of the directive antennas and a central node that makes use of a monopole antenna, it is established that the maximum separation distance between them is that at which the correctly received packets are lower than 100% of those sent. Finally, the communications performance of the wireless sensor nodes was assessed in a flat place featuring line of sight.

### III. RESULTS

This section presents the main outcomes of the proposed approach in terms of the node integration, antenna performance and comparison with current commercial solutions.

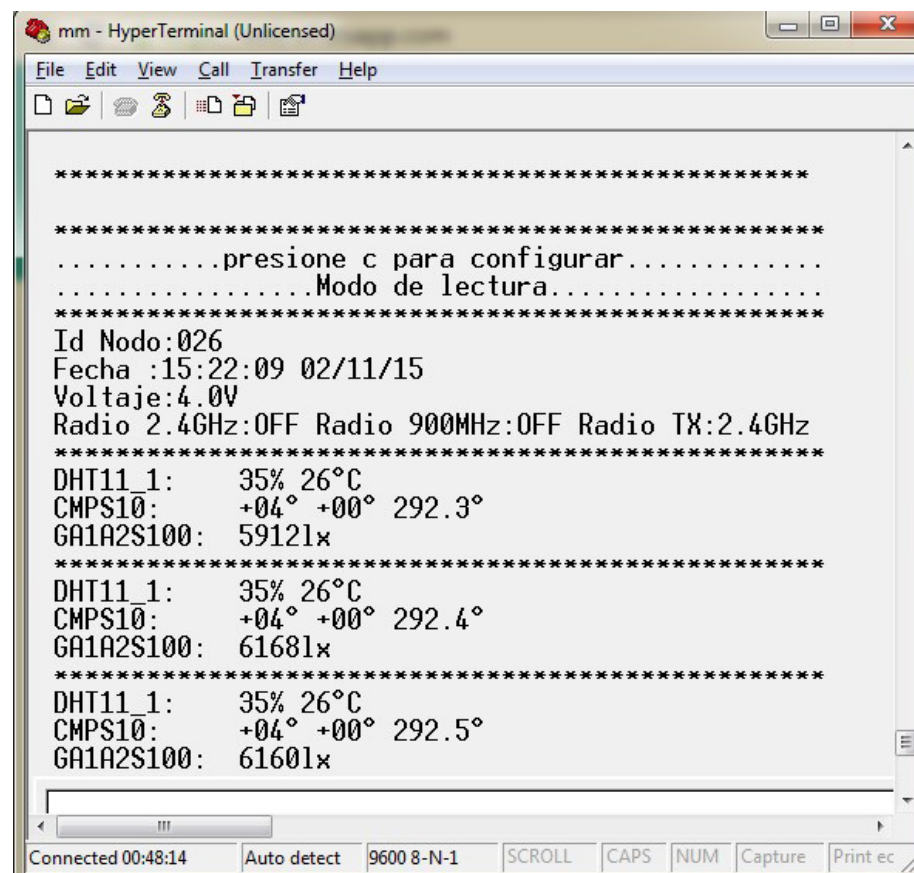
#### A. Node Results

Three operation modes allow the configuration, testing and monitoring in a quick and friendly way of the sensors and node characteristics through a RS232 connection. Fig. 4 shows the options of the configuration mode, Fig. 5 shows the data shown in the demo mode and Fig. 6 shows the results shown for the operation mode [18].



```
mm - HyperTerminal (Unlicensed)
File Edit View Call Transfer Help
Voltaje:4.1V
Radio 2.4GHz:OFF Radio 900MHz:OFF Radio TX:2.4GHz
*****
*****
.....MENU DE CONFIGURACION DEL NODO.....
01)LM35_1: OFF      02)LM35_2:  OFF
03)HIH_4000_1: OFF  04)HIH_4000_2: OFF
05)DHT11_1:  OFF   06)DHT11_2:  OFF
07)CMPS10:   OFF   08)PRESENCE: OFF
09)GP2Y0A02YK: OFF 10)HCSR04:   OFF
11)GA1A2S100: OFF
12)Id Nodo:000
13)Fecha :00:00:03 01/01/00
14)T Muestreo Demo(s):03
15)T Muestreo Trabajo(s):0003
16)Radio 2.4GHz:OFF
17)Radio 900MHz:OFF
18)Radio Tx:2.4GHz
19)MODO TRABAJO:
20)MODO DEMO:
DIGITE LA OPCION QUE DESEA CONFIGURAR (XX): _
Connected 00:06:21 Auto detect 9600 8-N-1 SCROLL CAPS NUM Capture Print ec
```

Fig. 4. Configuration mode.  
Source: Adapted from [18].



```
mm - HyperTerminal (Unlicensed)
File Edit View Call Transfer Help
.....presione c para configurar.....
.....Modo de lectura.....
*****
Id Nodo:026
Fecha :15:22:09 02/11/15
Voltaje:4.0V
Radio 2.4GHz:OFF Radio 900MHz:OFF Radio TX:2.4GHz
*****
DHT11_1: 35% 26°C
CMPS10: +04° +00° 292.3°
GA1A2S100: 59121x
*****
DHT11_1: 35% 26°C
CMPS10: +04° +00° 292.4°
GA1A2S100: 61681x
*****
DHT11_1: 35% 26°C
CMPS10: +04° +00° 292.5°
GA1A2S100: 61601x
Connected 00:48:14 Auto detect 9600 8-N-1 SCROLL CAPS NUM Capture Print ec
```

Fig. 5. Demo mode.  
Source: Adapted from [18].

```

mm - HyperTerminal (Unlicensed)
File Edit View Call Transfer Help
16)Radio 2.4GHz: OFF
17)Radio 900MHz: OFF
18)Radio Tx: 2.4GHz
19)MODO TRABAJO:
20)MODO DEMO:
DIGITE LA OPCION QUE DESEA CONFIGURAR (XX): 19

*****
026 15:33:53 02/11/15 3.9V 05)35% 25°C 07)+23° -03° 313.7° 11)58681x
026 15:33:57 02/11/15 3.9V 05)33% 25°C 07)+23° -03° 313.6° 11)61141x
026 15:34:01 02/11/15 3.9V 05)35% 25°C 07)+23° -02° 313.7° 11)61241x
026 15:34:05 02/11/15 3.9V 05)35% 25°C 07)+23° -03° 313.7° 11)61181x
026 15:34:09 02/11/15 3.9V 05)35% 25°C 07)+23° -03° 313.7° 11)61261x
026 15:34:13 02/11/15 3.9V 05)35% 25°C 07)+23° -02° 314.1° 11)61241x
026 15:34:17 02/11/15 3.9V 05)35% 25°C 07)+23° -03° 313.6° 11)61141x
026 15:34:22 02/11/15 3.9V 05)35% 25°C 07)+23° -03° 313.7° 11)61281x
026 15:34:26 02/11/15 3.9V 05)35% 25°C 07)+23° -03° 314.1° 11)61141x
026 15:34:30 02/11/15 3.9V 05)35% 25°C 07)+23° -03° 313.7° 11)61281x
026 15:34:34 02/11/15 3.9V 05)35% 25°C 07)+23° -02° 313.8° 11)61261x
026 15:34:38 02/11/15 3.9V 05)35% 25°C 07)+23° -03° 313.9° 11)61161x
026 15:34:42 02/11/15 3.9V 05)35% 25°C 07)+23° -03° 313.6° 11)61261x
026 15:34:46 02/11/15 3.9V 05)35% 25°C 07)+24° -03° 314.0° 11)61161x
-
Connected 00:59:30 Auto detect 9600 8-N-1 SCROLL CAPS NUM Capture Print echo

```

Fig. 6. Operation mode.  
Source: Adapted from [18].

The demo mode enables the user to test deactivated sensors by the configuration mode in order to know any eventual anomaly that is affecting the normal operation. In addition, it allows monitoring the other parameters previously mentioned. The information is displayed in an organized structure easy to read by the user. Finally, the operation mode displays the sensor and node information where the data units are sent as frames as shown in Fig. 6. Each frame shows the node ID, the date, the voltage of the node, followed by the sensor identification with their respective measured signal, e.g. sensor number 5 and sensor number 7 in Fig. 6. The use of frames facilitates reception, processing, storage in a central node and monitoring through an interface, as it will be used in a real environment [18].

### B. Antenna Results

In this section, the results of the measurements carried out for various antenna parameters are described. Fig. 7 shows the measured and simulated reflection coefficient ( $S_{11}$ ), in Fig. 8 is shown both the gain simulated and measured and in Fig. 9 the measured 2D radiation pattern is presented.

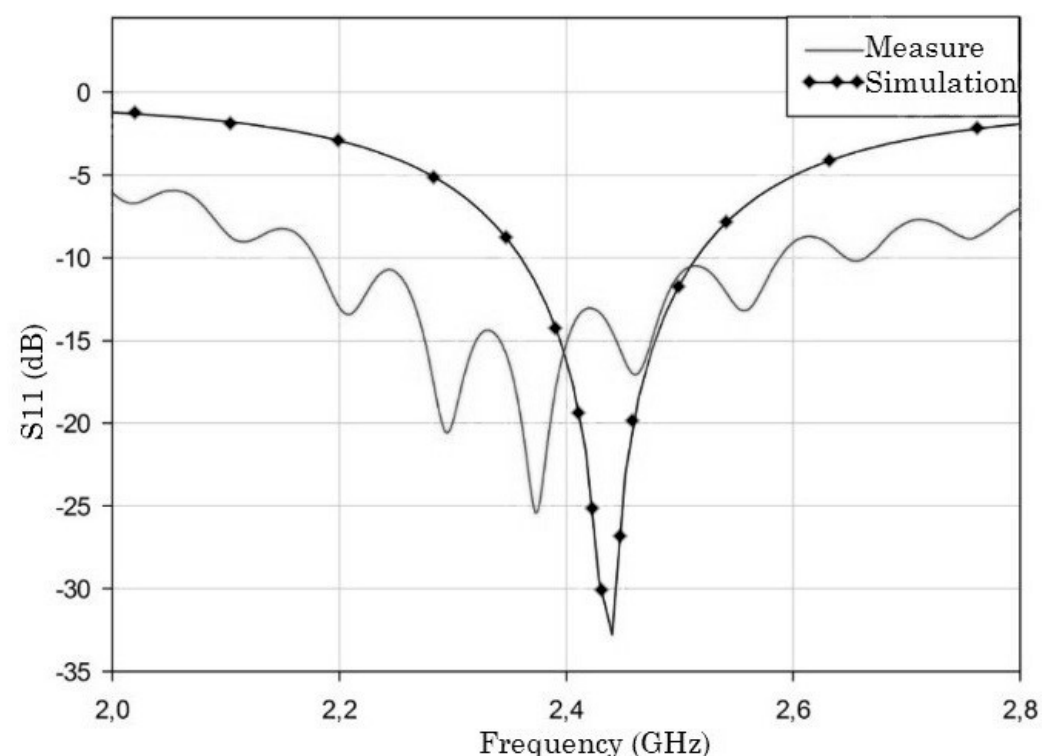


Fig. 7. Measured and simulated reflection coefficient ( $S_{11}$ ) of the SPA antenna.  
Source: Authors.



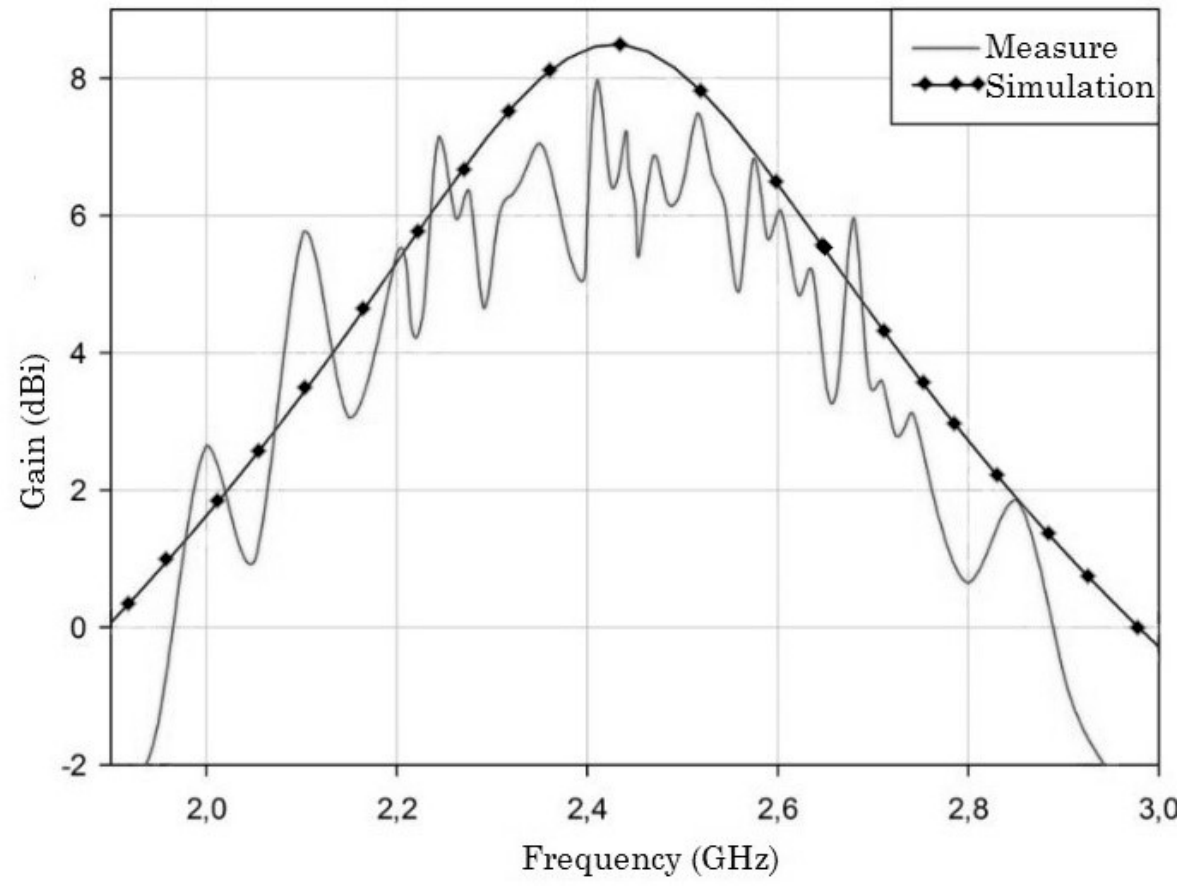


Fig. 8. Measured and simulated gain of the SPA antenna.  
Source: Authors.

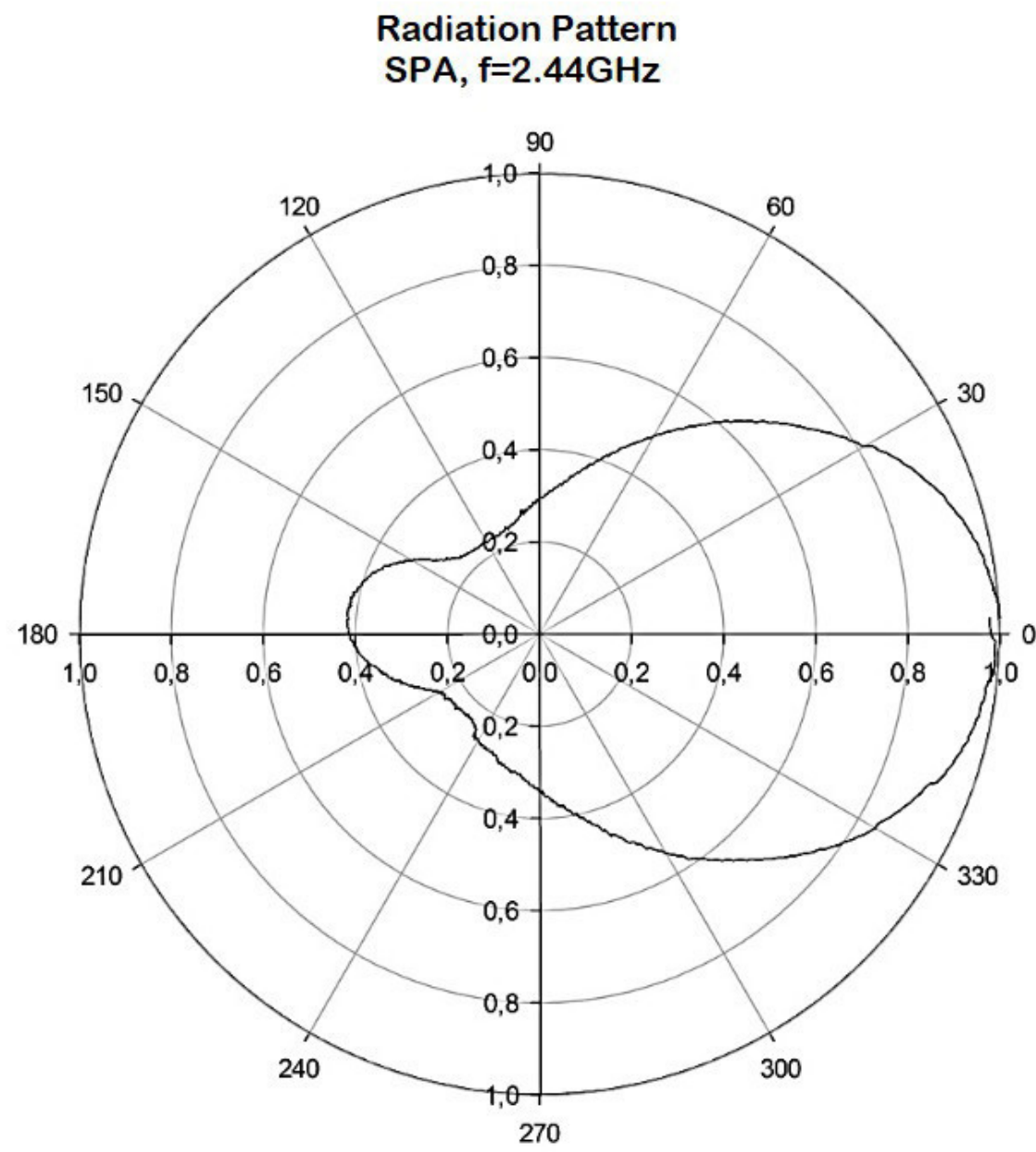


Fig. 9. Measured 2D radiation pattern of the SPA antenna at 2.44GHz.  
Source: Authors.

The result for the log periodic antenna is shown in Fig. 10 where the reflection coefficient is depicted. Fig. 11 presents a simulated and measured comparison regarding the gain and Fig. 12 and Fig. 13 show the measured 2D radiation pattern for 2.44 GHz and 915 MHz respectively.

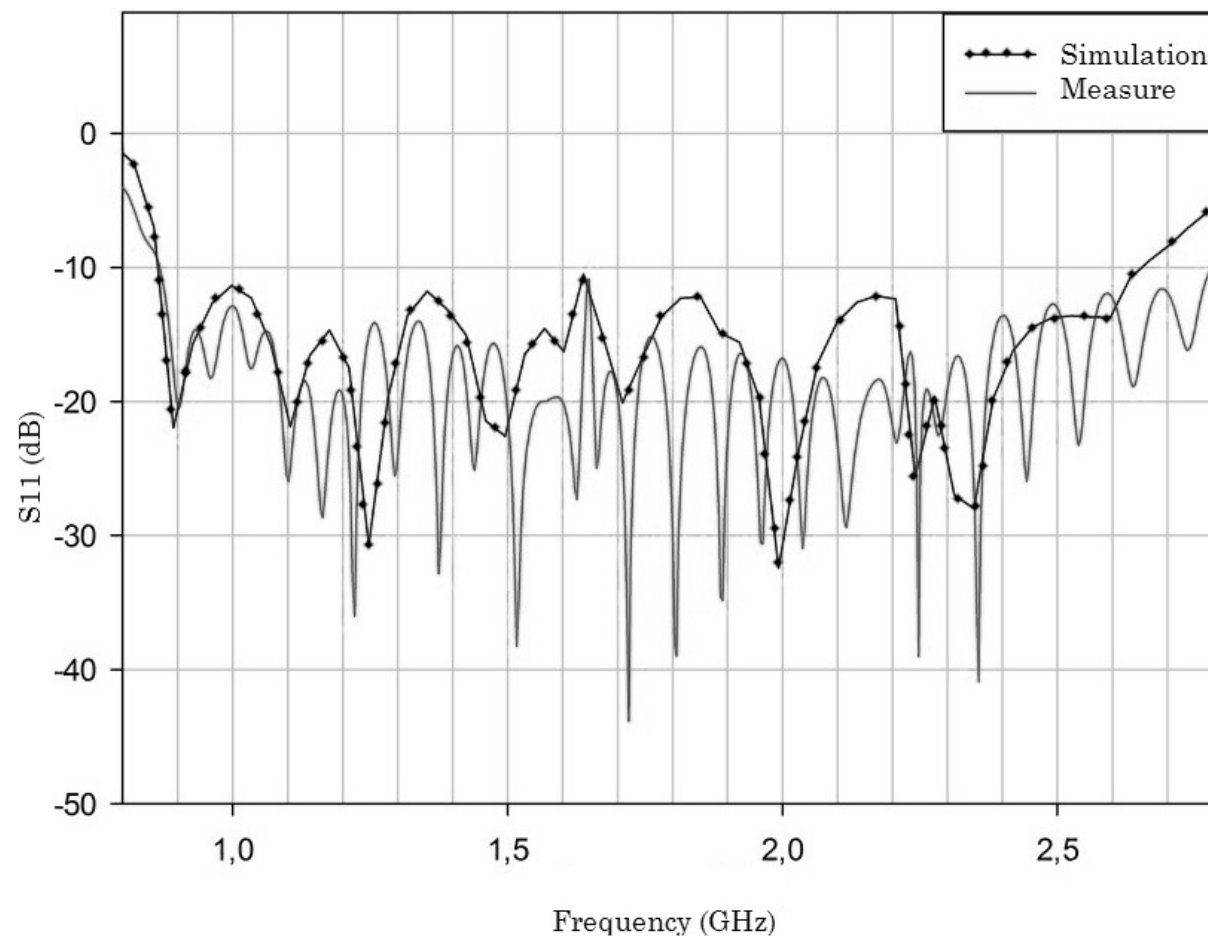


Fig. 10. Measured and simulated reflection coefficient ( ) of the log periodic antenna. Source: Authors.

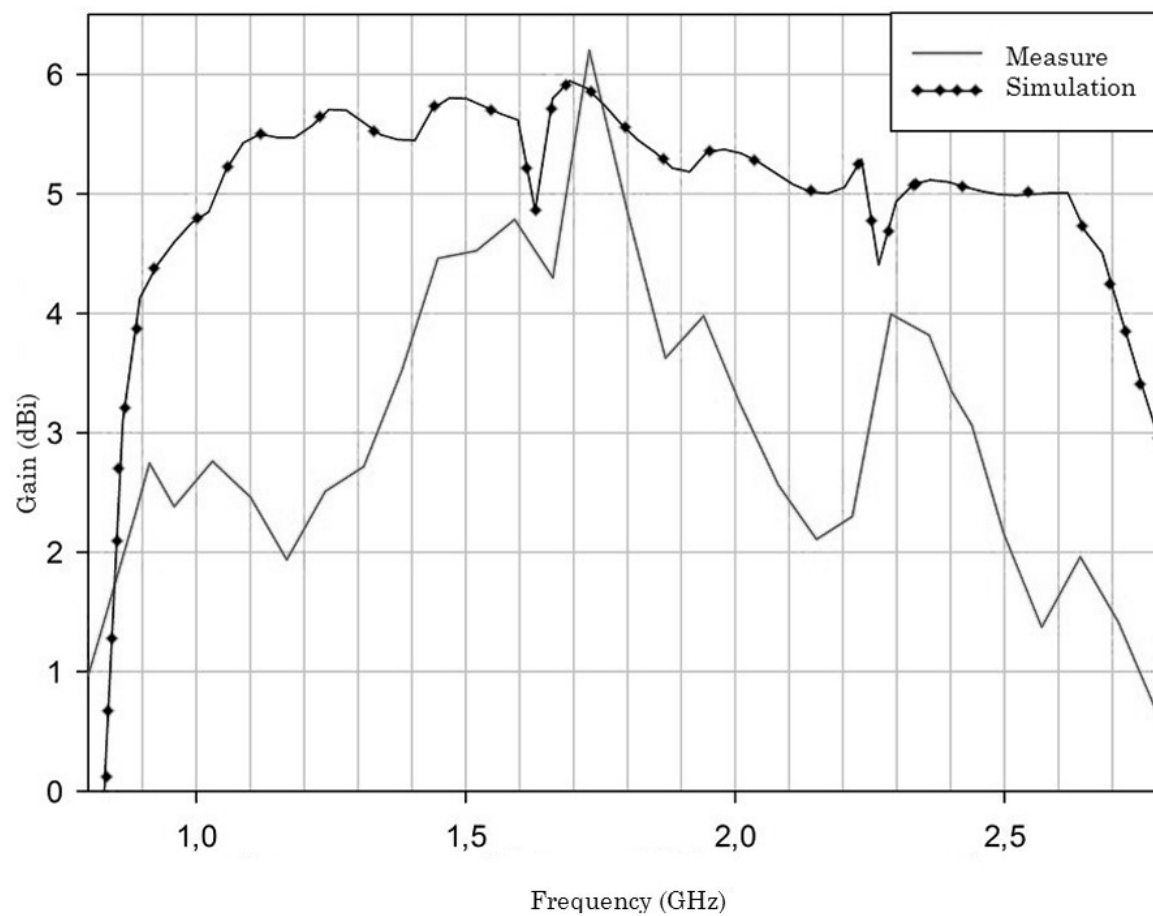


Fig. 11. Measured and simulated gain of the log periodic antenna. Source: Authors.

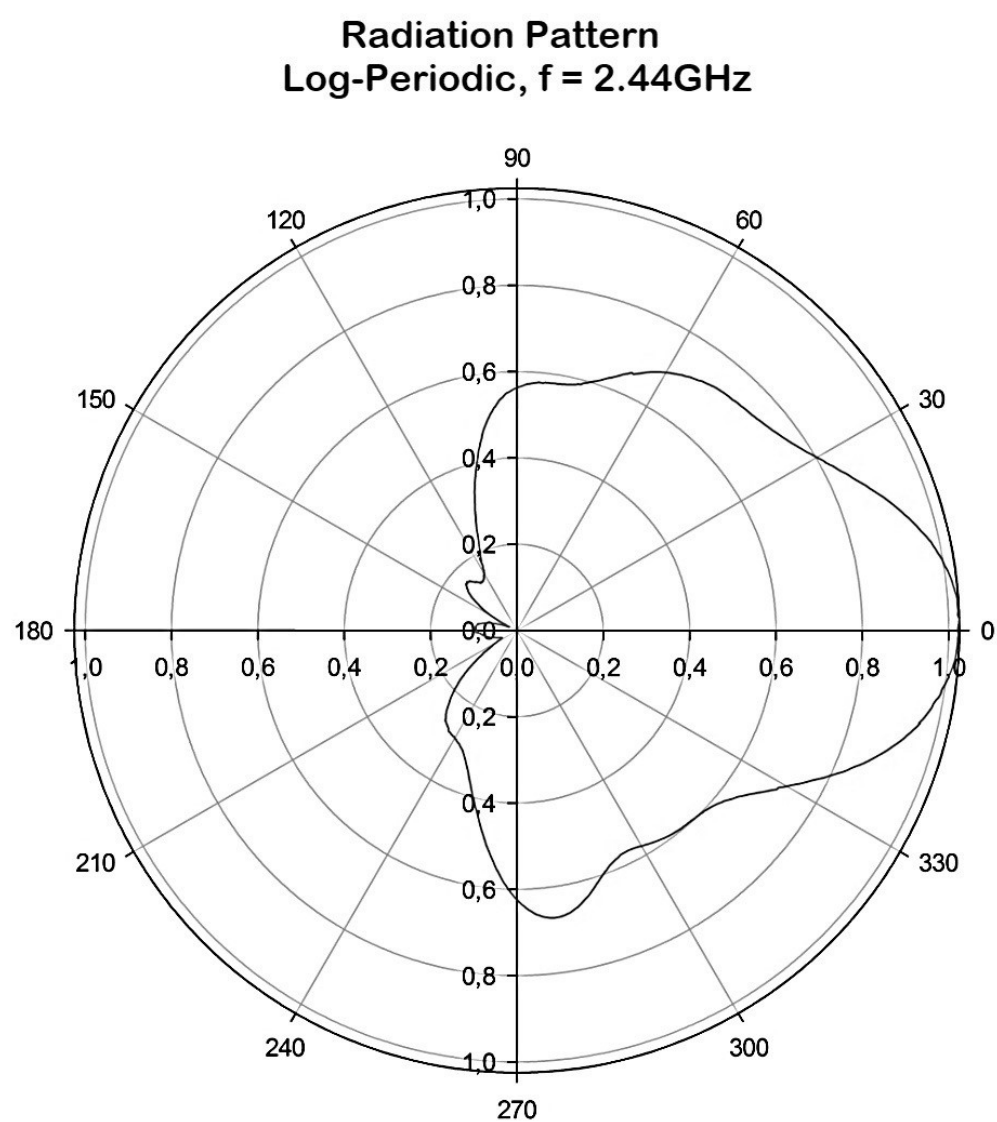


Fig. 12. Measured 2D radiation pattern of the log periodic antenna at 2.44 GHz.  
Source: Authors.

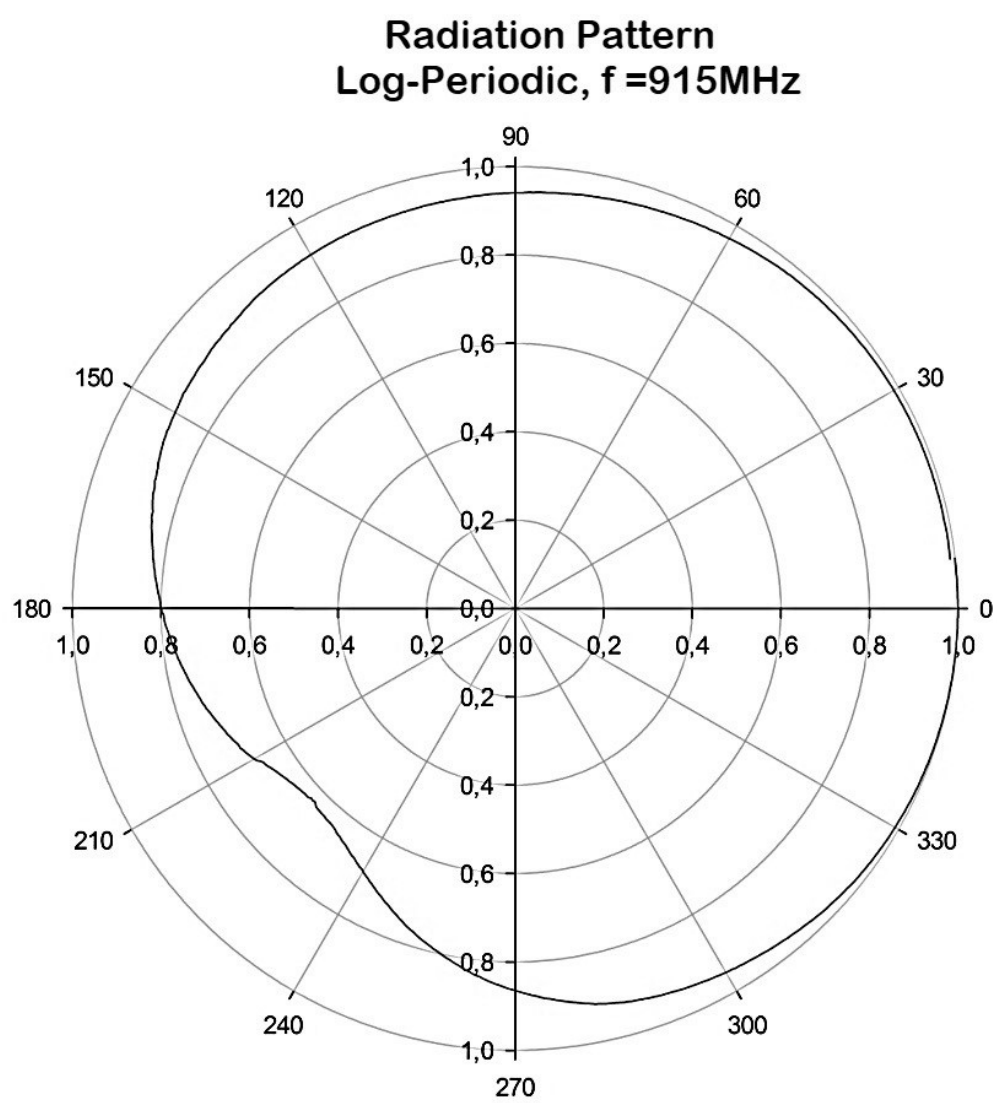


Fig. 13. Measured 2D radiation pattern of the log periodic antenna at 915 MHz.  
Source: Authors.

As far as the SPA antenna results are concerned, a 16.8% bandwidth was obtained; this represents a 6.58% higher than the value obtained in the simulations. However, 7.2 dBi gain was measured as compared with 8.48dBi simulated presenting a 15% of error. This antenna resonates from 2.18 GHz to 2.58 GHz at a reference of  $-10$  dB. Finally, the S11 measurement was  $-14.94$  dB at 2.44 GHz. The results for the log periodic antenna are better in terms of the obtained bandwidth. 3.196:1 was obtained in the experimental measurement and 3.048:1 was found in the simulations. A 3.06dBi gain at 2.44G Hz and 2.74 dBi at 915 MHz was measured. This antenna operates from 869MHz to 2.778 GHz at  $-10$ dB reference, the measured S11 was  $-24.65$  dB at 2.44 GHz and  $-15.17$  dB at 915 MHz [18].

### C. Reach

Results obtained regarding the transmission distance of the wireless sensor node are shown in Table 3. The table also compares the reached transmission distance of our approach with the transmission distance reported in the datasheets of commercial XBee radios.

TABLE 3. TRANSMISSION DISTANCE WITH SPA AND LOG-PERIODIC ANTENNAS.

XBee Model	Frequency	Antenna	Gain	Reach
ZB S2B	2.44 GHz	Monopole	1.5 dBi	169 m
Pro ZB S2C	2.44 GHz	Monopole	1.5 dBi	115 m
Pro ZB S2C	2.44 GHz	Chip	0.6 dBi	85 m
Pro XSC S3B	915 MHz	Log-Periodic	2.7 dBi	4.1 km
Pro S1	2.44 GHz	Log-Periodic	3.0 dBi	938 m
Pro S1	2.44 GHz	SPA	7.2 dBi	2.5 km

Source: Adapted from [18].

### D. Designed Node Comparison with Commercial Nodes

The main features of the approach presented in this paper are: significant increase in the transmission distance, multiple compatibility with dedicated sensors, possibility of including a large number sensor with different protocols and as a unique feature, the proposed node is the only one with simultaneous transmission at two different frequency bands. For comparison purposes, Table 4 and Table 5 describes the main features of the proposed approach (bold) against the characteristics of commercial solutions available on the market.

TABLE 4. COMMUNICATION SPECIFICATIONS OF WIRELESS SENSOR NODES.

Sensor Node	Antenna	Tx – Rx Frequency	Maximum Outdoor Scope
Waspnote	Monopole RPSMA (Xbee)	Depend on Xbee	Depend on Xbee
Lotus	Half Wave Dipole	2.4 GHz	500m
IMOTE2	Half Wave Monopole	2.4 GHz	30m
eZ430-RF2500	Onboard Antenna	2.4 GHz	Aprox. 50m
Designed at Double frequency	Log – Periodic bandwidth	2.4 GHz and 915 MHz	2,4G Hz: 1000 m 915 MHz: 4140 m
Designed at 2.4 GHz	SPA High gain and directive	2.4 GHz	2500m

Source: Authors.

TABLE 5. TECHNICAL SPECIFICATIONS OF WSN.

Sensor Node	Microcontrolller	Sensors
Wasmote	Atmel ATmega 1281	Compatible with 70 dedicated sensors.
°Lotus	LPC1758 Cortex M3 32 bits	Dedicated: light, temperature, RH, barometric, pressure, acceleration, acoustic, magnetic and other Memsec.
IMOTE2	ARM core Intel PXA271	No dedicated sensors of I2C, AC97, JTAG and Camera Chip Interface protocols.
eZ430-RF2500	TI MSP430F2274	3 dedicated sensors: temperature, humidity and light.
Designed at Double frequency	PSoC CY8CKIT-059	11 dedicated sensors and others with I2C, UART, SPI, One Wire, Digital I / O and Analog protocols.
Designed at 2.4 GHz	PSoC CY8CKIT-059	11 dedicated sensors and others with I2C, UART, SPI, One Wire, Digital I / O and Analog protocols.

Source: Authors.

#### IV. CONCLUSIONS

The wireless sensor node prototype designed with the SPA antenna at 2.44 GHz reached a 2.5 km communication link distance due to the 7.2 dBi gain and directive radiation pattern. This fact represents a significant achievement in the 2.4GHz band compared to commercial solutions. The sensor node with log periodic antenna reached the outstanding distance of 4.14 km at 915 MHz; this is attributed to the band frequency properties and antenna performance. The advantage of this approach relies on the possibility to operate on both frequency bands (2.44 GHz and 915 MHz) by selecting the appropriate band according to network and application needs. It was evidenced that the features offered by the PSoC technology facilitate the construction of sensor devices prototypes because it includes a large number of analog and digital peripherals that enables signal processing without additional components. This fact results in reduction of costs and space on implementations. The proposed node allows connecting an Xbee with log periodic or SPA antenna as a radiating element, the central processing unit based on the PSoC is configured by the user who can change the operation frequency evaluating aspects such as distance and interferences. This node represents an approach for an accessible device in terms of cost and configuration, contributing to the deployment of wireless sensor networks.

Wireless sensor nodes based on directive antennas demonstrate the feasibility to implement the frequency and space diversity as a solution to mitigate multipath signal loss, environmental fading and interference of signals in plantations and forests, improving the effectiveness of such systems for future smart agriculture applications.

#### ACKNOWLEDGMENTS

This investigation makes part of “Diseño de agrupación circular de haz conmutado para aplicaciones en estimación de Dirección de Arribo (DOA)” project. The authors wish to thank and acknowledge Colciencias and Universidad Distrital Francisco José de Caldas for the economic support on this investigation and for encouraging research in Colombia.

#### REFERENCES

- [1] W. Dargie & C. Poellabauer, *Fundamentals of Wireless Sensor Networks*, N. Y., USA: John Wiley & Sons Ltd, 2010. <https://doi.org/10.1002/9780470666388>
- [2] S. M. N. Shruthi & A. Habtewolde, “Energy Harvesting System Based WSN Application Using ARM7 Controller,” presented at *Int. Conf. Smart Technol. Smart Nation*, Smart. Tech. Con., Blr. Ind., pp. 1388–1392, 17-19 Aug. 2017. <https://doi.org/10.1109/SmartTechCon.2017.8358593>
- [3] R. Ashby, *Designer’s Guide to the Cypress PSoC?* Burlington, MA, USA: Newnes, 2005. <https://doi.org/10.1016/B978-075067780-6/50005-2>
- [4] S. Ali, A. Ashraf, S. B. Qaisar, M. K. Afridi, H. Saeed, S. Rashid, E. A. Felemban & A. A. Sheikh, “SimpliMote: A Wireless Sensor Network Monitoring Platform for Oil and Gas Pipelines,” *IEEE Syst. J.*, vol. 12, no. 1, pp. 1–12, Aug. 2016. <https://doi.org/10.1109/JSYST.2016.2597171>
- [5] T. Savic, “WSN Architecture for Smart Irrigation System,” *23rd International Scientific-Professional Conference on Information Technology*, IT, Zbk, Me., pp.1–4, 19-24 Feb. 2018. <https://doi.org/10.1109/SPIT.2018.8350859>
- [6] Olimex, “XBee IO Pro,” *guadalinux.org*, 2006. Available: <https://www.mcielectronics.cl/shop/product/mci-xbee-io-pro-v2-arduino-leonardo-compatible-mci-electronics-11014?search=XBee+IO+Pro>

- [7] J. Edwards, F. Demers, M. St-Hilaire & T. Kunz, "Comparison of ns2.34's ZigBee/802.15.4 implementation to Memsic's IRIS Motes," presented at *7th Int. Wirel. Commun. Mob. Comput. Conf., IWCMC*, Ist., Tr., pp. 986–991, 12 Aug. 2011. <https://doi.org/10.1109/IWCMC.2011.5982675>
- [8] T. Instruments, "eZ430-RF2500," *Texas Instruments*, [online], 2015. Available: <http://www.ti.com>
- [9] B. Road & E. Minnetonka, "Product Manual 90000938-A," *XBee-PRO® XSC RF Module*, Digi. Int., Mtk., USA., 2008. Available: <https://www.sparkfun.com/datasheets/Wireless/Zigbee/XBee-XCS-Manual.pdf>
- [10] Digi International, "Digi XBee® 802.15.4," *Digi.com*, [online], 2009. Available: <http://www.digi.com/products/wireless-wired-embedded-solutions/zigbee-rf-modules/point-multipoint-rfmodules/xbee-series1-module#specs>
- [11] Digi International, "XST-AN019a," *XBee & XBee-PRO OEM RF Module Antenna Considerations*, Digi Int., Mtk., USA., Jun., 2012. Available: [http://ftp1.digi.com/support/images/XST-AN019a\\_XBeeAntennas.pdf](http://ftp1.digi.com/support/images/XST-AN019a_XBeeAntennas.pdf)
- [12] S. Khairunniza-Bejo, N. Ramli & F. M. Muharam, "Wireless Sensor Network (WSN) Applications in Plantation Canopy Areas: A Review," *Asian J Sci Res*, vol. 11, no. 2, pp. 151–161, 2018. <https://doi.org/10.3923/ajsr.2018.151.161>
- [13] T. Rama Rao, D. Balachander, N. Tiwari & P. MVSN2, "Ultra-high frequency near-ground short-range propagation measurements in forest and plantation environments for wireless sensor networks," *IET Wirel Sens Syst*, vol. 3, no. 1, pp. 80–84, 2013. <https://doi.org/10.1049/iet-wss.2012.0059>
- [14] D. Balachander, T. Rama Rao & G. Mahesh, "RF Propagation Investigations in Agricultural Fields and Gardens for Wireless Sensor Communications," *IEEE Conference on Information and Communication Technologies, ICT*, Thuckalay, Ind., 11-12 Apr. 2013. <https://doi.org/10.1109/CICT.2013.6558195>
- [15] X. Feng, F. Yan & X. Liu, "Study of Wireless Communication Technologies on Internet of Things for Precision Agriculture," *Wirel Pers Commun*, vol. 108, pp. 1785–1802, May. 2019. <https://doi.org/10.1007/s11277-019-06496-7>
- [16] Y. Ai, M. Cheffena, T. Ohtsuki, & H. Zhuang, "Secrecy Performance Analysis of Wireless Sensor Networks," *IEEE Sens Lett*, vol. 3, no. 5, pp. 1–4, 4 Apr. 2019. <https://doi.org/10.1109/LSENS.2019.2909323>
- [17] B. Kusy, C. Richter, W. Hu, M. Afanasyev, R. Jurdak, M. Brünig, D. Abbott, C. Huynh & D. Ostryt, "Radio diversity for reliable communication in WSNs," *ACM/IEEE International Conference on Information Processing in Sensor Networks*, ACM/IEEE, Chi., IL, USA., pp. 270–281, 12–14 Apr. 2011. Available: <https://ieeexplore.ieee.org/document/5779044>
- [18] M. Gonzalez, C. Echeverry, G. Puerto & C. Suárez-Fajardo, "Design and implementation of wireless sensor node in 900MHz and 2.4GHz bands," *IEEE Colombian Conference on Communications and Computing, COLCOM*, Ctg., Co., pp. 1–5, Apr. 27-29, 2016. <https://doi.org/10.1109/Col-ComCon.2016.7516393>
- [19] Z. N. Chen and M. Y. W. Chia, *Broadband Planar Antennas: Design and Applications*. NJ, USA: John Wiley & Sons Ltd, 2006.
- [20] W. O. Coburn and S. A. McCormick, "The Effect of Fabrication Tolerances on a Suspended Plate Antenna," presented at *International Applied Computational Electromagnetics Society Symposium, ACES*, Flr., It., 2017. <https://doi.org/10.23919/ROPACES.2017.7916283>
- [21] C. A. Suárez-Fajardo, *Introducción al análisis y diseño de antenas planas y sus aplicaciones*. Bg., Co.: Ediciones Udistrital, 2017.
- [22] C. A. Balanis, *Antenna Theory: Analysis and Design*. N.Y., USA: John Wiley & Sons Ltd, 2005.
- [23] D. E Isbell, "Log Periodic Dipole Array Antenna," *IRE Trans Antennas Propag*, vol. 8, no. 3, pp. 260–267, May. 1969. <https://doi.org/10.1109/TAP.1960.1144848>

**Martha Gonzalez Jaramillo.** Bachelor degree in electronic engineering and specialization in Engineering Project Management at the Universidad Distrital Francisco José de Caldas (Colombia). She was a young researcher with Colciencias in GRECO research group. <https://orcid.org/0000-0001-9503-8885>

**Cesar Echeverry Moreno.** Bachelor degree in electronic engineering in Universidad Distrital Francisco José de Caldas (Colombia). Currently he is pursuing a masters degree in Strategic Planning and Technology Management in the Universidad Popular Autonoma del Estado de Puebla (México). <https://orcid.org/0000-0002-3063-5125>

**Carlos Suárez Fajardo.** MSc. and PhD. degrees in Telecommunications from the Universidad Politécnica de Valencia (Valencia, Spain), for which he joined the electromagnetic radiation group (GRE) of the university. Currently holds the position of full Professor at the Universidad Distrital Francisco José de Caldas (Bogotá, D.C., Colombia). Up to date, he has published more than 50 papers in international journals and conferences in the field of antennas. His research interests include wideband and multi-band planar antennas, microwave engineering, Metamaterial applications and small satellite communication systems. <https://orcid.org/0000-0002-1460-5831>

**Gustavo Puerto Leguizamón.** Telecommunications Engineer. In 2003, he joined the Group of Optical and Quantum Communications of the Universidad Politécnica de Valencia (Spain). Ph.D. in Telecommunications and postdoctoral researcher at the Institute of Telecommunications and Multimedia Applications at the same university until 2011. Currently associate professor at the Universidad Distrital Francisco José de Caldas (Bogotá, D.C., Colombia). Up to date, he has published more than 50 articles in international journals and conferences in the field of optical networks. He is evaluator of Colciencias and of the journals IEEE Journal on Lightwave Technologies, IEEE Photonic Technology Letters and Optics Express. His research interests include radio over fiber systems, optical networking and optical access networks. <https://orcid.org/0000-0002-6420-9693>